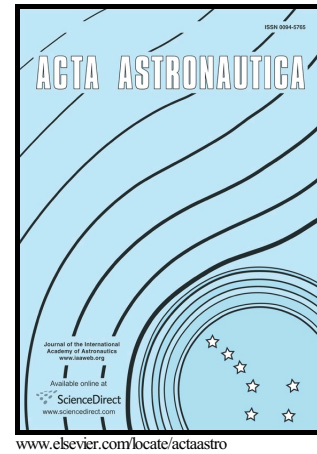


# Author's Accepted Manuscript

Asteroid retrieval missions enabled by invariant manifold dynamics

Joan Pau Sanchez, Daniel Garcia Yáñez



PII: S0094-5765(15)30363-5  
DOI: <http://dx.doi.org/10.1016/j.actaastro.2016.05.034>  
Reference: AA5843

To appear in: *Acta Astronautica*

Received date: 30 December 2015

Accepted date: 26 May 2016

Cite this article as: Joan Pau Sanchez and Daniel Garcia Yáñez, Asteroid retrieval missions enabled by invariant manifold dynamics, *Acta Astronautica* <http://dx.doi.org/10.1016/j.actaastro.2016.05.034>

This is a PDF file of an unedited manuscript that has been accepted for publication. As a service to our customers we are providing this early version of the manuscript. The manuscript will undergo copyediting, typesetting, and review of the resulting galley proof before it is published in its final citable form. Please note that during the production process errors may be discovered which could affect the content, and all legal disclaimers that apply to the journal pertain.

## Asteroid Retrieval Missions Enabled by Invariant Manifold Dynamics

Joan Pau Sanchez<sup>a</sup>, Daniel García Yáñez<sup>b</sup><sup>a</sup>Space Research Group, Centre of Autonomous and Cyber-Physical Systems, Cranfield University, MK43 0AL, Bedfordshire, United Kingdom<sup>b</sup>Institute of Space and Astronautical Science, Japan Aerospace eXploration Agency, Sagami-hara, Japan.

jp.sanchez@cranfield.ac.uk

daniel.yarnoz@ac.jaxa.jp

**Abstract**

Near Earth Asteroids are attractive targets for new space missions; firstly, because of their scientific importance, but also because of their impact threat and prospective resources. The asteroid retrieval mission concept has thus arisen as a synergistic approach to tackle these three facets of interest in one single mission. This paper reviews the methodology used by the authors (2013) in a previous search for objects that could be transported from accessible heliocentric orbits into the Earth's neighbourhood at affordable costs (or Easily Retrievable Objects, a.k.a. EROs). This methodology consisted of a heuristic pruning and an impulsive manoeuvre trajectory optimisation. Low thrust propulsion on the other hand clearly enables the transportation of much larger objects due to its much higher specific impulse. Hence, in this paper, low thrust retrieval transfers are sought using impulsive trajectories as first guesses to solve the optimal control problem. GPOPS-II is used to transcribe the continuous-time optimal control problem to a nonlinear programming problem (NLP). The latter is solved by IPOPT, an open source software package for large-scale NLPs. Finally, a natural continuation procedure that increases the asteroid mass allows to find out the largest objects that could be retrieved from a given asteroid orbit. If this retrievable mass is larger than the actual mass of the asteroid, the asteroid retrieval mission for this particular object is said to be feasible. The paper concludes with an updated list of 17 EROs, as of April 2016, with their maximum retrievable masses by means of low thrust propulsion. This ranges from 2,000 tonnes for the easiest object to be retrieved to 300 tonnes for the least accessible of them.

Keywords: Asteroid missions, Easily Retrievable Objects, trajectory design, low thrust, Libration-point orbits

**1. INTRODUCTION**

Recently, significant interest has been devoted to the understanding of the minor bodies of the Solar System, including near-Earth and main belt asteroids and comets. NASA, ESA and JAXA have conceived a series of missions to obtain data from such bodies, having in mind that their characterisation not only provides a deeper insight into the Solar System but also represents a technological challenge for space exploration. Near Earth objects (NEOs), in particular, have also stepped into prominence because of two important aspects: they are among the easiest celestial bodies to reach from the Earth and they may represent a threat to our planet.

As witnesses of the early Solar System, NEOs could cast some light into the unresolved questions about the formation of planets from the pre-solar nebula, and perhaps settle debates on the origin of water on Earth or panspermian theories, among others (e.g., [1, 2]). This scientific importance has translated into an increasing number of robotic probes sent to NEOs, and many more planned for the near future. Their low gravity well have also identified them as the only “planetary” surface that can be visited by crewed missions under NASA's flexible path plan [3]. Science however is not the only interest of these objects and mission concepts exploring synergies with science, planetary protection and space resources utilization have started to be uttered. Examples of this are recent NASA and ESA studies on a kinetic impact demonstration mission on a binary object, DART and AIM [4].

Proposed technologies and methods for the deflection of Earth-impacting objects have experienced significant advances, along with increasing knowledge of the asteroid population. While initially devised to mitigate the hazard posed by global impact threats, the current impact risk is largely posed by the population of small undiscovered objects [5], and thus methods have been proposed to provide subtle changes to the orbits of small objects, as opposed to large-scale interventions such as the use of nuclear devices [6]. This latter batch of deflection methods, such as the low thrust tugboat [7], gravity tractor [8], ion beam [9] or small kinetic impactor [10] are moreover based on currently proven space technologies. They can therefore render the apparently ambitious scenario of manipulating asteroid trajectories a likely option for the near future.

On the other hand, the in-situ utilisation of resources in space has long been suggested as the means of lowering the cost of space missions, for example, by providing bulk mass for radiation shielding or manufacturing propellant for interplanetary transfers [11]. The development of technologies for in-situ resource utilisation (ISRU) could become a potentially disruptive innovation for space exploration and utilisation and, for example, enable large-scale space ventures that could today be considered far-fetched, such as large space solar power satellites, sustaining communities in space or geoengineering [12]. Although the concept of asteroid mining dates back to the early rocketry pioneers [13], evidences of a renewed interest in the topic can be found in the growing body of literature [14-16], as well as in high profile private enterprise ventures such as by Planetary Resources Inc. [17].

With regards to the accessibility of asteroid resources, recent work by Sanchez and McInnes [18] discusses how a substantial quantity of resources could potentially be accessed at relatively low energy; on the order of  $10^{14}$  kg of material could be harvested at an energy cost lower than that required to access resources from the surface of the Moon. More importantly, asteroid resources could be accessed across a wide spectrum of energies, and thus, current technologies could be adapted to return to the Earth's neighbourhood small objects from 2 to 30 meters diameter for scientific exploration and resource utilisation purposes [18].

Together with the availability of small objects in the Earth's orbital vicinity, recent advances in invariant manifold dynamics (e.g., [19]) provide the necessary tools to design surprisingly low energy trajectories, which may in turn enable the possibility to retrieve small celestial objects from their natural heliocentric trajectories. An asteroid retrieval mission envisages a spacecraft that rendezvous with an asteroid, lassos it and then hauls it back to Earth neighbourhood [20]. Current interplanetary spacecraft however have masses on the order of  $10^3$  kg, while an asteroid of 10 meters diameter will most likely have a mass of the order of  $10^6$  kg. Hence, moving such a large object, with the same ease that scientific payload is transported today, would demand propulsion systems order of magnitudes more powerful and efficient; or alternatively, orbital transfers orders of magnitude less demanding than those to reach other planets in the Solar System. Hence, it is here that invariant manifolds associated with periodic and quasi-periodic orbits near the Sun-Earth  $L_1$  and  $L_2$  points provide important pathways to design extremely low energy transfers.

This paper reports on the latest results from AsteroidRetrieval Project (PIEF-GA-2012-330649<sup>\*</sup>). The project aimed at gaining further understanding of the current and near-term capability to modify the asteroid's trajectory by judicious use of orbital mechanics. More particularly, the project focused on exploiting the subtle underlying dynamics of multi-body systems, in order to benefit from simultaneous gravitational interactions between the Sun, Earth and Moon to find effective means to transport asteroid material to the Earth's vicinity. The paper will also review the earlier work by García Yáñez et al. [21], which presented a new sub-category of NEOs in an attempt to provide an objective and quantifiable classification of asteroids that could be transported from accessible heliocentric orbits into the Earth's neighbourhood at affordable costs.

Section 2 will briefly describe fundamental aspects of low energy transport phenomena in multi-body systems. The methodology used to distinguish between those asteroids that can be "*easily*" transported back to Earth vicinity and those that cannot is then discussed in Section 3, and was originally presented in García Yáñez et al. [21]. The list of potential candidates for retrieval, as of 12<sup>th</sup> April 2016, is given in Section 4, together with their optimized impulsive capture trajectories. The latter set of solutions is then used as first guesses to solve the low thrust optimal control problem, which is described in Section 5. The opportunities and potential retrieval capability enabled by invariant manifold dynamics associated with periodic and quasi-periodic orbits in the Sun-Earth system is finally discussed and compared with published results from NASA's Asteroid Redirect Robotic Mission (ARRM) [22] (Section 6).

## 2. LOW ENERGY TRANSPORT CONDUITS

Solar system transport phenomena, such as the rapid orbital transitions experienced by comets Oterma and Gehrels 3, from heliocentric orbits outside Jupiter orbital radius to orbits enclosed by it [23], or the Kirkwood gaps in the main asteroid belt, are some manifestations of the sensitivities of multi-body dynamics. The hyperbolic invariant manifold structures associated with periodic orbits near the  $L_1$  and  $L_2$  collinear points of the Three Body Problem provide a mathematical representation of the mechanism that controls the aforementioned transport phenomena [23-25]. The same underlying principles that enable these transport phenomena allow also for excellent opportunities to design incredibly low energy transfers.

### 2.1. Periodic and Quasi-Periodic orbits

This paper thus focuses on the dynamics near the Sun-Earth  $L_1$  and  $L_2$  points, as they are the gate keepers for ballistic capture of asteroids in the Earth's vicinity. The paper assumes the motion of the spacecraft and asteroid

<sup>\*</sup> [http://cordis.europa.eu/project/rcn/108052\\_en.html](http://cordis.europa.eu/project/rcn/108052_en.html)

under the gravitational influence of the Sun and Earth within the framework of the Circular Restricted Three Body Problem (CR3BP). Thus, in a synodic reference frame centred in the barycentre of the Sun-Earth system, the unpropelled motion of the asteroid-hauling spacecraft can be modelled by [26, 27]:

$$\begin{aligned}\ddot{x} &= -2\dot{y} + \frac{\partial\Omega}{\partial x} \\ \ddot{y} &= 2\dot{x} + \frac{\partial\Omega}{\partial y} \\ \ddot{z} &= \frac{\partial\Omega}{\partial z}\end{aligned}\quad (0)$$

where the potential function  $\Omega$  is defined as:

$$\Omega = \frac{x^2 + y^2}{2} + \frac{1-\mu}{r_S} + \frac{\mu}{r_E} \quad (0)$$

where  $r_S$  and  $r_E$  are the distances to the Sun and the Earth respectively and the mass parameter  $\mu$  considered in the paper is  $3.0032080443 \times 10^{-6}$ , which neglects the mass of the Moon. Note that the usual normalised units are used when citing Jacobi constant values [26].

Together with the five well-known equilibrium positions of Eq.(0), from which  $L_1$  and  $L_2$  points are the two closest to the Earth, respectively defined as in Figure 1, an extensive catalogue of bounded motion near these equilibria has also been comprehensively mapped (e.g., [28]). The principal families of these are planar and vertical families of Lyapunov periodic orbits, quasi-periodic Lissajous orbits, and periodic and quasi-periodic halo orbits [29]. Although, some other families of periodic orbits can be found by exploring bifurcations in the aforementioned main families [28]. This paper however presents capture or retrieval opportunities enabled by three classes of periodic motion near the Sun-Earth  $L_1$  and  $L_2$  points: These are planar and vertical Lyapunov and halo orbits, from now on referred to as a whole as libration point orbits (LPOs).

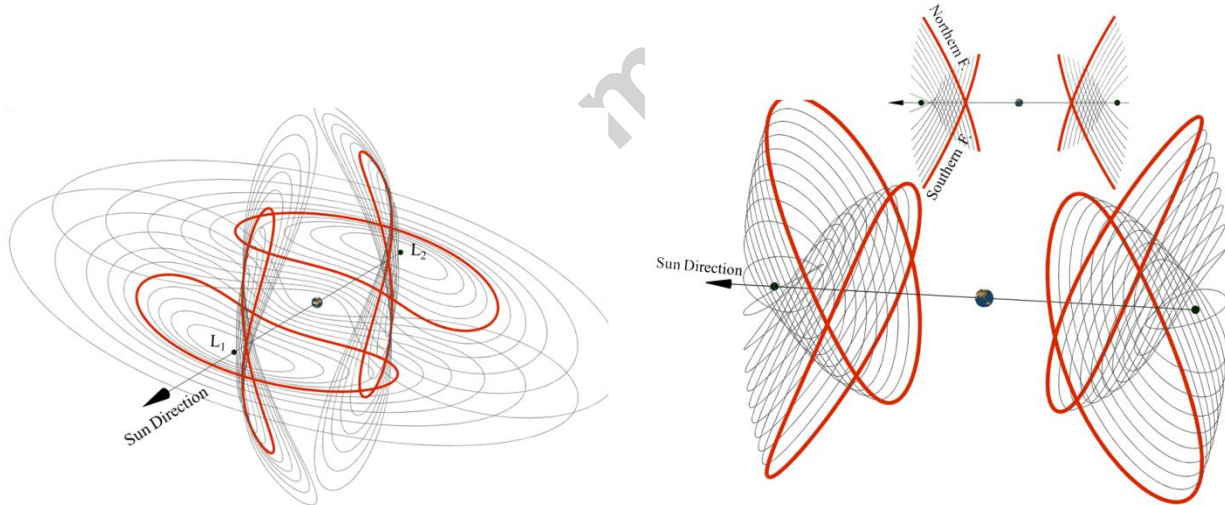


**Figure 1.** Series of planar and vertical Lyapunov orbits (left) and northern and southern halo orbits (right) associated with the Sun-Earth  $L_1$  and  $L_2$  points. Lyapunov orbits are plotted ranging from Jacobi constant 3.0007982727 to 3.0000030032. Halo orbits are plotted ranging from Jacobi constant of 3.0008189806 to 3.0004448196. The thicker red line corresponds to a Jacobi constant of 3.0004448196, which corresponds to half the distance between the energy at equilibrium in  $L_2$  and  $L_3$ , at the corresponding  $\mu$ .

Ideally, an asteroid transported into one of these orbits would remain near the libration point for an indefinite time. In practice, however, these orbits are unstable, and an infinitesimal deviation from the periodic orbit will make the asteroid depart asymptotically from the libration point regions. Nevertheless, small correction manoeuvres can be planned to keep the asteroid in the vicinity of the periodic orbit [30, 31]. Indeed, for example, the  $\Delta v$  budget for station-keeping of the James Webb Space Telescope near the Sun-Earth  $L_2$  point is much smaller than the standard station-keeping budget for geostationary satellites [32].

## 2.2. Invariant Manifold Dynamics

In fact, the instability associated with these classes of bounded motion near the collinear libration points brings certain benefits to the possibility of transporting asteroid material into them. The linear behaviour of the motion near

the collinear libration points is of the type *centre x centre x saddle* [27]. This particular dynamical behaviour ensures that, inherent to any bounded trajectory near the collinear libration points, an infinite number of trajectories exist that asymptotically approach, or depart, from the bounded motion. Each set of trajectories asymptotically approaching, or departing, a periodic or quasi-periodic orbit near the  $L_1$  or  $L_2$  points forms a hyperbolic invariant manifold structure.

There are two classes of invariant manifolds: the central invariant and the hyperbolic invariant. The central invariant manifold is composed of periodic and quasi-periodic orbits near the libration points, while the hyperbolic invariant manifold consists of a stable and an unstable set of trajectories associated to the central invariant manifold near an equilibrium point. The unstable manifold is formed by the infinite set of trajectories that exponentially leaves a periodic or quasi-periodic orbit belonging to the central invariant manifold to which they are associated. The stable manifold, on the other hand, consists of an infinite number of trajectories exponentially approaching the periodic or quasi-periodic orbit.

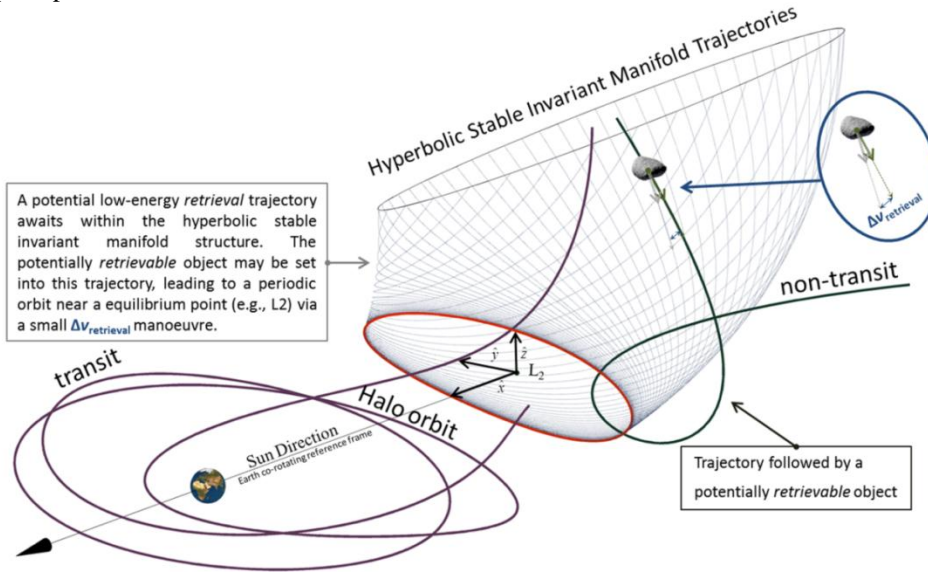


**Figure 2.** Schematic representation of the four categories of motion near the  $L_2$  point (represented by the set of axes in the figure): periodic motion around  $L_2$  (i.e., halo orbit), hyperbolic invariant manifold structure (i.e., set of stable hyperbolic invariant manifold trajectories), transit trajectory and non-transit trajectory. Also, an asteroid retrieval opportunity enabled by the invariant manifold structure is depicted by the small  $\Delta v$  necessary to change the motion of an asteroid in a non-transit trajectory to a trajectory that asymptotically reached the halo orbit.

It is well known that the phase space near the equilibrium regions can be divided into four broad classes of motion; bound motion near the equilibrium position (e.g., periodic as shown in Figure 1), asymptotic trajectories that approach or depart from the latter, transit trajectories, and, non-transit trajectories (see Figure 2). A transit orbit is a trajectory such that its motion undergoes a rapid transition between orbital regimes, e.g., heliocentric and planetocentric. In the Sun-Earth case depicted in Figure 2, for example, the transit trajectory approaches Earth following a heliocentric trajectory, transits through the bottle neck delimited by the halo orbit and becomes temporarily captured at the Earth. An important observation from dynamical system theory is that the hyperbolic invariant manifold structure defined by the set of asymptotic trajectories forms a phase space separatrix between transit and non-transit orbits.

As illustrated in Figure 2, an asteroid retrieval opportunity benefits from the insights provided by the stable invariant manifold structures, associated with a given LPO, in such a way that with relatively little manoeuvring (only a single small burn in the example shown in Figure 2) an asteroid may be placed into a trajectory that asymptotically reaches an equilibrium configuration near the Sun-Earth  $L_1$  and  $L_2$  points. It also follows from the aforementioned four categories of motion near the libration points that periodic orbits near the Sun-Earth  $L_1$  and  $L_2$  points can also be targeted as natural gateways of low energy trajectories to Earth-centred temporarily captured trajectories or transfers to other locations of the cislunar space, such as the Earth-Moon Lagrangian points [33, 34].

### 3. EASILY RETRIEVABLE OBJECTS

Given the opportunities underlined above for low cost retrieval of asteroids, it is yet to be defined the number of suitable candidates within the known population of these objects. This section then describes the search for *easily retrievable objects* among the surveyed population of asteroids as of 12<sup>th</sup> April 2016. The term easily retrievable objects (EROs) was originally defined in García-Yárnoz et al. [21], and refers to objects whose orbits could be modified into an stable hyperbolic trajectory by means of at most two impulsive manoeuvres with a combined cost below 500 m/s. A systematic search for EROs is now carried out, selecting the  $L_1$  and  $L_2$  regions as the target destination for the captured material.

### 3.1. Invariant Manifold Trajectories leading to $L_1$ and $L_2$

In order to provide a simple but robust method for categorizing EROs, the design of the transfer from the asteroid orbit to the  $L_1$  and  $L_2$  LPO consists of a ballistic arc, with two impulsive burns at the start and end, intersecting a hyperbolic stable invariant manifold asymptotically approaching the desired periodic orbits. Note that this work then considers only the inbound leg of a full capture mission.

Planar Lyapunov, vertical Lyapunov, and halo orbits around  $L_1$  and  $L_2$  generated with the methods described in the previous section were considered as target orbits. The invariant stable manifold trajectories were computed by perturbing the target orbit periodic solutions around the Lagrangian point on the stable eigenvector direction with a magnitude of  $10^{-6}$  in normalized units [26]. These initial conditions were propagated backwards in the Circular Restricted 3-Body Problem (Eq.(0)) until they reached a desired fixed section in the Sun-Earth rotating frame. We refer to this backward propagation time as the manifold transfer time  $t_m$ . The section was arbitrarily selected as the one forming an angle of  $\pm\pi/8$  with the Sun-Earth line ( $\pi/8$  for  $L_2$  orbits, see Figure 3, the symmetrical section at  $-\pi/8$  for those targeting  $L_1$ ). This corresponds roughly to a distance to Earth of the order of 0.4 AU, where the gravitational influence of the planet can be considered small. No additional perturbations were considered in the backward propagation.

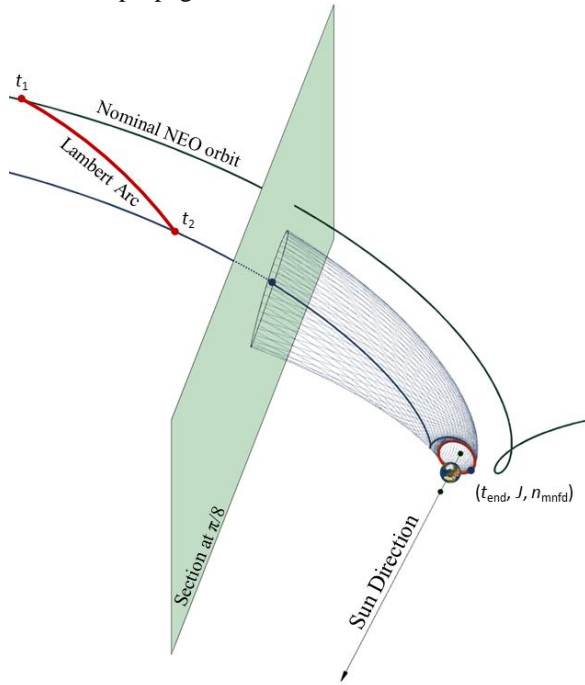


**Figure 3.** Schematic representation of a transfer to  $L_2$ .

In this analysis, the Earth is assumed to be in a circular orbit 1 AU away from the Sun. This simplification allows the conditions of the manifold trajectories (and in particular in the selected section) to be independent of the insertion time into the final orbit. The only exception is the longitude of the perihelion, i.e., the sum of the right ascension of the ascending node  $\Omega$  and the argument of perihelion  $\omega$ , which varies with the insertion time with respect to a reference time with the following relation:

$$(\Omega + \omega) = (\Omega_{REF} + \omega_{REF}) + \frac{2\pi}{T}(t - t_{REF}) \quad (1)$$

where  $\Omega_{REF}$  and  $\omega_{REF}$  are the right ascension of the ascending node and the argument of perihelion at the  $\pm\pi/8$  section for an insertion into a target orbit at reference time  $t_{REF}$ , and  $T$  is the period of the Earth. For orbits with non-zero



inclination, the argument of perihelion of the manifolds is also independent of the insertion time and the above equation indicates a variation in  $\Omega$ . However, in the case of planar Lyapunov with zero inclination,  $\Omega$  is not defined and an arbitrary value of zero can be selected, resulting in the equation representing a change in argument of perihelion.

A large database of conditions  $(a, e, i, \Omega_{\text{REF}}, \omega_{\text{REF}}, M)$  at the target section was then generated. The purpose of the database is to store beforehand all relevant data, in order to avoid large computational costs during the optimization of the capture trajectories. It was verified that if a sufficiently accurate discretization of all the capture conditions was performed, any hyperbolic trajectory within the infinite set in the invariant manifold could be quickly estimated by interpolating the stored data. Hence,  $10^6$  sets of  $(a, e, i, \Omega_{\text{REF}}, \omega_{\text{REF}}, M)$  were generated that covered the eight different target LPOs (i.e. 4 at each libration point) for a range of Jacobi constants as shown in Figure 1. In other words, sets of  $(a, e, i, \Omega_{\text{REF}}, \omega_{\text{REF}}, M)$  were generated and used as bullseye to target asteroids into the hyperbolic trajectories associated with all the periodic orbits shown in Figure 1.

The transfer between the NEO orbit and the manifold is then calculated as a heliocentric Lambert arc of a restricted two-body problem with two impulsive burns, one to depart from the original NEO orbit, the final one for insertion into the manifold, with the insertion constrained to take place before or at the  $\pm\pi/8$  section in the synodic reference frame.

Thus, within the framework described above, an impulsive capture transfer can be uniquely defined with only five design variables. These are, as shown Figure 3, the time of the Lambert arc departure manoeuvre  $t_1$ , the time of the Lambert insertion manoeuvre  $t_2$ , the insertion date at the target periodic orbit  $t_{\text{end}}$ , the energy of the final orbit  $J$ , and a fifth parameter that determines the insertion point of the manifold transfer along the target periodic orbit  $n_{\text{mnfd}}$ . This last three design parameters  $(t_{\text{end}}, J, n_{\text{mnfd}})$  uniquely determine a target hyperbolic trajectory represented as a Keplerian set  $(a, e, i, \Omega_{\text{REF}}, \omega_{\text{REF}}, M)$  for a given type of LPO and libration point.

The total  $\Delta v$  change, composed by the departure and insertion manoeuvres  $(\Delta v_1, \Delta v_2)$ , can then be used as the performance index of the transfer. A single objective optimization problem has now been defined, in which ideally the set of design variables  $(t_1, t_2, t_{\text{end}}, J, n_{\text{mnfd}})$  that minimize the transfer cost  $\Delta v_{\text{total}}$  are sought for each asteroid. Note also that this optimization problem targets one single asteroid into the hyperbolic stable invariant manifold associated with one specific type of periodic orbit (either vertical, planar Lyapunov or halo) at one of the two collinear equilibrium points ( $L_1, L_2$ ). Hence, the same optimization problem needs to be repeated for each equilibrium point considered and target periodic orbit (i.e., sixfold).

### 3.2. Asteroid Catalogue Pruning

The NEO population known on 12<sup>th</sup> April 2016 is composed by 14,166 objects. The ephemerides of all these objects were downloaded from the Minor Planets Center Database<sup>†</sup>.

Performing for each known asteroid a single objective optimization as that described in previous section would entail high computational costs. However, this is clearly not necessary, since only a small portion of all the known asteroids would make good candidates for retrieval. The issue then is to use simple heuristic rules to resolve the candidates that may have a minimum potential to become good candidates, from those that can be completely discarded.

As an integral of motion in the CR3BP, the Jacobi Constant can provide a first guess of the suitability of an asteroid to be captured [35]. If the Jacobi Constant of an asteroid diverges excessively from that of the target hyperbolic trajectories, then it would also mean that the energy costs to retrieve the asteroid would be high. The Jacobi constant  $J$  of an asteroid in the Sun-Earth system can be approximated with the Tisserand parameter as:

$$J \approx \frac{1}{a} + 2\sqrt{a(1-e^2)}\cos i \quad (2)$$

where  $a$ ,  $e$  and  $i$  are the semi-major axis (in AU), eccentricity and inclination of the asteroid orbit, respectively.

Figure 4 represents the complete range of different hyperbolic invariant manifolds used as target capture trajectories. These are represented in terms of its Jacobi Constant, but also in terms of perihelion and aphelion radius, as well as inclination, for the two collinear points. The figure illustrates the proximity of a much reduced set of asteroids (represented as crosses) to the capture manifolds. Note that among the 14,166 objects, only 77 have a Jacobi Constant ranging within [2.9992, 3.001], but once periapsis, apoapsis and inclination are also accounted for only 5 objects are plotted. It is also worth noting that asteroid 2006 RH120 has been highlighted, due to its proximity to the  $L_2$  manifolds. From these graphs and ignoring any phasing issues, 2006 RH120 can already be identified as a good retrieval mission candidate, as its perihelion and aphelion radius are close to or within the range of all three

<sup>†</sup> <http://www.minorplanetcenter.org/>

types of considered manifolds, and its inclination also lies close to the halo orbit manifolds. The manifold orbital elements appear to be a good filter to prune the list of NEOs to be captured.

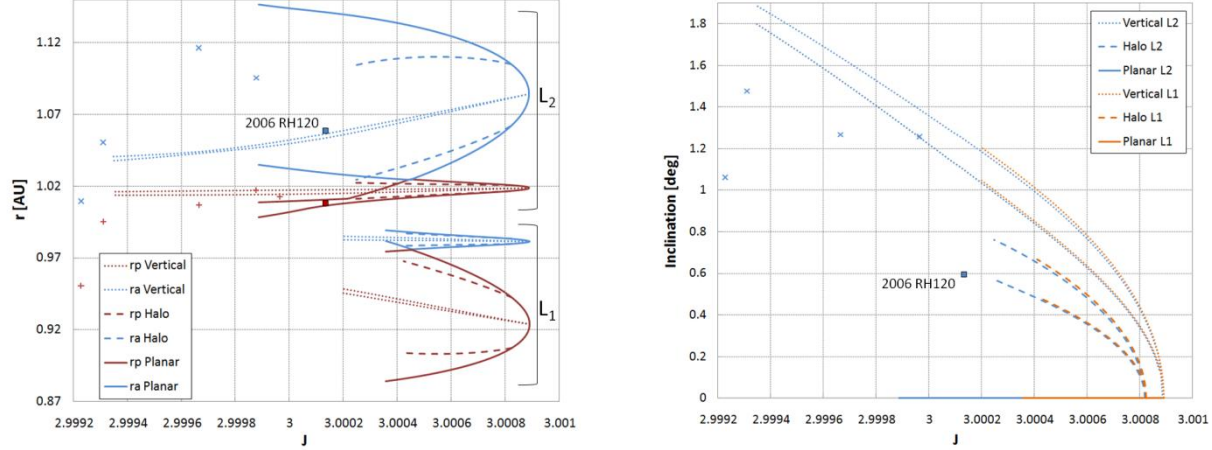


**Figure 4.** Minimum and maximum perihelion and aphelion radius (left) and inclination (right) of the manifolds leading to planar Lyapunov, vertical Lyapunov and halo orbits around  $L_1$  and  $L_2$ , as a function of Jacobi Constant  $J$ .

Aside from the discussion on Figure 4, a more systematic filter is thus devised. As a first approximation of the expected total cost in terms of  $\Delta v$ , a bi-impulsive cost prediction with both burns assumed at aphelion and perihelion was implemented. Either of the two burns is also responsible for correcting the inclination. The  $\Delta v$  required to modify the apsides can be expressed as:

$$\Delta v_a = \sqrt{\mu_s \left( \frac{2}{r} - \frac{1}{a_f} \right)} - \sqrt{\mu_s \left( \frac{2}{r} - \frac{1}{a_0} \right)} \quad (3)$$

where  $\mu_s$  is the Sun's gravitational constant,  $r$  is the distance to the Sun at which the burn is made (perihelion or aphelion distance),  $a_0$  and  $a_f$  are the initial and final semimajor axis before and after the burn. On the other hand, the  $\Delta v$  required to modify the inclination at either apsis can be approximated by:

$$\Delta v_i = 2 \sqrt{\frac{\mu_s}{a_0}} r^* \sin(\|i_t - i_0\| / 2) \quad (4)$$

where  $\|i_t - i_0\|$  is the absolute magnitude of the difference between the initial inclination of the asteroid  $i_0$  and the inclination of the target hyperbolic trajectory  $i_t$ , and  $r^*$  corresponds to the ratio of perihelion and aphelion distance if the burn is performed at aphelion, or its inverse if performed at perihelion. The total  $\Delta v_t$  of the capture trajectory can then be estimated as:

$$\Delta v_t = \sqrt{\Delta v_{a1}^2 + \Delta v_{i1}^2} + \sqrt{\Delta v_{a2}^2 + \Delta v_{i2}^2} \quad (5)$$

with one burn performed at each of the apsides, and one of the two inclination change  $\Delta v$  assumed zero. The estimated transfer  $\Delta v$  corresponds to the minimum of four cases: aphelion burn modifying perihelion distance as well as inclination followed by a perihelion burn modifying only the aphelion distance; perihelion burn modifying aphelion distance and inclination followed by an aphelion burn modifying only perihelion distance; and two more equivalent sequences with the only difference that the inclination change is done during the second burn instead. Eq.(5) provides only a very rough approximations, intended for pruning unlikely candidates from the large asteroid database. In particular, it implicitly assumes that the line of nodes coincides with the line of apsides, and thus the inclination change can be performed at one of the apsides. Also, these formulas only take into consideration the shape and inclination of the orbits, ignoring any phasing with the Earth.

Note finally that in order to obtain a  $\Delta v$  estimate from Eq.(5) both the initial  $(a_0, e_0, i_0)$  of the asteroid orbit and the target  $(a_t, e_t, i_t)$  of the hyperbolic trajectory are needed. The minimum  $\Delta v_t$  is then computed for each asteroid targeting each one of the  $10^6$  possible capture trajectories generated previously. The results of this are described in the following section.

#### 4. ASTEROID RETRIEVAL OPPORTUNITIES

The analytical  $\Delta v$  estimate described by Eq.(5) was used to filter the original population of 14,166 objects to only 33 potential candidates. A threshold  $\Delta v$  cost of 700 m/s was used to prune out all likely unsuitable targets. Although, the appropriateness of the threshold was difficult to assess beforehand, it was later confirmed that none of the 33



candidates yielded optimized ballistic capture transfers with costs substantially below that indicated by the filter. The complete list of filtered candidates is reproduced in Table 1.

Table 1. List of remaining asteroid after pruning.

2006 RH120	2007 UN12	2012 TF79	2011 BL45	2010 VQ98	2011 UD21	2012 LA	2010 UE51
2008 EA9	2013 RZ53	2008 UA202	2000 SG344	2011 MD	2009 BD	1991 VG	2014 QN266
2014WU200	2010 UJ	2013 GH66	2011 BQ50	2006 QQ56	2001 GP2	2008 HU4	2012 WR10
2008 JL24	2014WA366	2010 JW34	2013 BS45	2006 JY26	2015 XZ378	2015 VC2	2015 JD3
2015 KK57							

For each of the potentially retrievable NEOs in Table 1, feasible capture transfers with arrival dates in the interval 2020-2100 were obtained. More accurate ephemerides were downloaded for each asteroid from JPL's Horizon system<sup>‡</sup>. The ephemerides consisted in sets of osculating Keplerian elements ranging from 2020-2100. However, since the first guess generation of retrieval transfers is here based in a Lambert arc optimization, transfers were computed only for the first complete synodic period on which the asteroid is outside regions where the Earth's gravitational effect plays an important role. These are, as described earlier, the regions with angular distance from the Sun-Earth line larger than  $\pi/8$  radians. The Keplerian elements of each asteroid were then taken as the osculating elements furthest from the Earth during the synodic period of the first Lambert transfer opportunity.

The Lambert transfers between the asteroid initial orbit and the hyperbolic target transfers were optimised using EPIC, a global optimisation method that uses a stochastic search blended with an automatic solution space decomposition technique [36]. Single objective optimisations with total transfer  $\Delta v$  as the cost function were carried out. Trajectories obtained with EPIC were then locally optimised with MATLAB's built-in constrained optimisation function *fmincon*. Lambert arcs with up to 3 complete revolutions before insertion into the manifold were considered. For cases with at least one complete revolution, the two possible solutions of the Lambert problem were optimised. This implies that 7 full problem optimisations needed to be run for each potential NEO. In order to limit the total duration of the transfers, the insertion into the manifold was arbitrarily constrained to take place not earlier than 1000 days before the  $\pm\pi/8$  section during the global search. This constraint was released in the local optimisation.

Table 2 summarises the optimized results for all objects for which transfers below 500 m/s were found. The  $\Delta v$  reported in the table are the minimum achieved transfer cost to capture a given asteroid into each different LPO orbit. Note however that the result of the global optimization is an extensive database of capture opportunities, all with different time of flight, departure date, etc, and yet relatively similar  $\Delta v$ . Also, it is important to highlight that the earliest departure time allowed for the transfers reported in Table 2 is the 1<sup>st</sup> January 2020. This is an important difference with the impulsive transfers reported in Garcia-Yarnoz et al [21], and it is the cause of some of the differences between the two tables.

As shown in the table, the average size of all the objects with potential to be retrieve is of 10 meters diameter. This is clear indicative that asteroids that can be easily transported to Earth vicinity are rare, and they can only be found among the numerous population of extremely small objects. Nevertheless, the sizes reported in Table 2 are only based in the rough approximation given by the following relation [37]:

$$D = 1329 \times 10^{-H/5} p_v^{-1/2} \text{ [km]} \quad (6)$$

where the absolute magnitude  $H$  is obtained from NEODys<sup>§</sup>, and the albedo  $p_v$  may range from 0.05, for very dark objects, to 0.5 for very bright objects [38].

<sup>‡</sup> <http://ssd.jpl.nasa.gov/?horizons>

<sup>§</sup> <http://newton.dm.unipi.it/neodys/>

**Table 2.** NEOs with ballistic transfer trajectories below 500 m/s as of asteroid database on 12<sup>th</sup> April 2016. The type of transfer is indicated by a 1 or 2 indicating L<sub>1</sub> or L<sub>2</sub> plus the letter P for planar Lyapunov, V for vertical Lyapunov, and Hn or Hs for north and south halo.

Rank #		a [AU]	e	i [deg]	H	Diameter [m]	Type	$\Delta v$ [km/s]
1	2006 RH120	1.033	0.024	0.595	29.50	2.4-7.5	2Hs	0.059
							2Hn	0.107
							2V	0.187
							2P	0.298
							2V	0.182
2	2010 VQ98	1.023	0.027	1.475	28.20	4.3-13.6	2Hn	0.393
							2Hs	0.487
							2P	0.195
3	2007 UN12	1.049	0.059	0.235	28.70	3.4-10.8	2Hs	0.271
							2Hn	0.327
							2V	0.434
4	2010 UE51	1.071	0.072	0.59	28.30	4.1-13.0	2Hs	0.405
							2P	0.348
5	2012 TF79	1.050	0.038	1.001	27.40	6.2-19.7	2Hn	0.273
							2V	0.282
6	2013 RZ53	1.016	0.028	2.123	31.30	1.1-3.6	2V	0.270
							2Hn	0.297
7	2014 WX202	1.036	0.059	0.413	29.63	2.2-7.0	2Hs	0.402
							2P	0.337
8	2008 EA9	1.059	0.080	0.424	27.70	5.4-17.1	2P	0.341
							1Hs	0.347
9	2011 UD21	0.980	0.030	1.062	28.50	3.8-11.9	1V	0.204
							1Hn	0.300
10	2008 UA202	1.033	0.069	0.264	29.40	2.5-7.8	2Hn	0.438
							2P	0.367
11	2015 PS228	1.057	0.084	0.439	28.80	3.3-10.3	2P	0.395
12	2009 BD	1.062	0.052	1.267	28.10	4.5-14.3	2Hn	0.395
							2V	0.487
13	2011 BL45	1.033	0.069	3.049	27.00	7.5-23.7	2V	0.395
14	2011 MD	1.056	0.037	2.446	28.00	4.7-14.9	2V	0.431
15	1991 VG	1.027	0.049	1.445	28.50	3.8-11.9	2Hs	0.453
							1P	0.470
16	2000 SG344	0.978	0.067	0.111	24.70	21.6-68.2	1Hs	0.487
							1Hn	0.500
17	2015 JD3	1.058	0.008	2.719	25.6	14.3-45.1	2V	0.496

## 5. LOW THRUST ASTEROID RETRIEVAL

The asteroids and capture trajectories summarized in Table 2 provide only the impulsive  $\Delta v$  costs of the retrieval trajectories. As such, they convey little understanding on the feasibility to retrieve these asteroids with current or near-term space technology. In order to obtain a first estimate of the mass and size of the asteroids that could be potentially captured, we need to consider also the basic mass budget of the spacecraft responsible to haul the asteroid back to Earth. Clearly then, the most relevant mission design for this is that of NASA's Asteroid Redirect Robotic Mission (ARRM) concept [22], which is still largely based on the original proposal by Keck's Asteroid Retrieval Feasibility Study [20]. The current design for NASA's ARRM envisages a mission capable to deliver a space system with the ability to *grab* a small asteroid and use a high power (~40 kW) solar electric propulsion to push the asteroid back to Earth vicinity. ARRM spacecraft dry mass  $m_{dry}$  is of 5,500 kg, a launch mass of about 18 tonnes, and an outbound transfer leg, i.e., Earth to asteroid, such that the spacecraft reaches the target asteroid with still about 10 tonnes of propellant that would be used to haul the asteroid back to Earth's vicinity. Hence, these figures are also used in the remaining of the paper.

Since the trajectories in Table 2 are impulsive approximations, given the spacecraft mass budget mentioned above and assuming a standard high-thrust propulsion system (Isp~300s), a quick estimate of the retrievable mass from each capture trajectory can be computed by means of Tsiolkovsky's rocket equation. Table 3 summarises the set of impulsive trajectories used to compute this first estimate of retrievable mass and the asteroid mass that could be retrieved with an Isp of 300s and impulsive manoeuvres. Note that the trajectories shown in Table 3 may differ

slightly from those reported in Table 2, i.e. marginally higher  $\Delta v$ . The reasons for these will be clear in the following paragraphs.

**Table 3.** Capture trajectories and retrievable mass estimates in impulsive transfer approximation.

Asteroid name		Orbit destination	Date [yyyy/mm/dd]			Energy of Manifold	Total Duration [yrs]	Δv [m/s]			Isp=300s retribable mass [t]
			Asteroid departure	Manifold insertion	L <sub>1/2</sub> arrival			Dep	Ins	Total	
1.	2006 RH120	2Hs	2021/02/04	2021/02/01	2028/08/05	3.000421	7.50	58	0	59	488
2.	2010 VQ98	2V	2028/12/12	2033/01/09	2037/10/23	3.000072	8.86	204	5	209	130
3.	2007 UN12	2P	2028/09/22	2032/2/13	2036/08/20	2.999887	7.91	15	180	195	140
4.	2010 UE51	2P	2027/07/08	2030/12/17	2035/12/18	2.999887	8.45	40	309	349	74
5.	2012 TF79	2Hn	2020/11/15	2024/08/01	2028/03/04	3.000249	7.30	42	238	280	95
6.	2013 RZ53	2V	2045/01/14	2048/08/25	2054/04/06	2.998840	9.22	200	91	291	91
7.	2014 WX202	2Hn	2023/12/05	2028/04/03	2031/08/24	3.000598	7.72	282	15	297	89
8.	2008 EA9	2P	2025/12/24	2030/4/26	2034/04/30	3.000158	8.35	112	245	357	72
9.	2011 UD21	1V	2032/08/19	2036/06/28	2040/10/28	3.000160	8.19	39	165	204	134
10.	2008 UA202	2P	2036/09/23	2040/11/08	2045/08/01	2.999887	8.85	202	165	367	70
11.	2015 PS228	2P	2033/02/01	2036/09/05	2041/06/07	2.999887	8.35	62	347	409	62
12.	2009 BD	2Hn	2028/11/27	2032/08/25	2036/05/11	3.000291	7.45	269	144	413	61
13.	2011 BL45	2V	2024/01/24	2027/06/10	2032/11/24	2.998570	8.84	106	345	451	55
14.	2011 MD	2V	2033/03/27	2037/02/17	2041/10/16	2.998680	8.56	407	25	431	58
15.	1991 VG	2Hs	2028/12/11	2032/03/12	2037/02/22	3.000249	8.20	401	53	454	54
16.	2000 SG344	1P	2054/05/11	2057/05/02	2061/06/27	3.000357	7.13	240	230	470	52
17.	2015 JD3	2V	2034/11/23	2038/10/12	2043/09/30	2.998846	8.85	134	410	543	44

Although a high thrust propulsion system has clear advantages, the tenfold excess velocity of the exhaust gases in the ionized plasma of low thrust propulsion systems would likely be a much more valuable benefit here. On the other hand, while a low thrust engine may use up to 10 times less propellant than its high-thrust counterpart, the key issue for the latter is how large an asteroid can be pushed given the low acceleration and the available transfer time. Hence, to solve these issues, low thrust retrieval trajectories are now sought for all the transfer options reported in Table 2. The power available for the low thrust system is assumed to be  $\sim 40$  kW [22]. This yields a maximum thrust capability of nearly 2 N with thrust efficiencies in the order of 70% [39]. A propulsion system specific impulse of  $\sim 3000$ s [22] is assumed.

### 5.1. Low Thrust Transfer Design

Low thrust trajectories are now sought using the first guess provided by the high thrust optimized results. The departure conditions are thus fixed to those obtained in the high thrust solutions, and summarized in Table 3. The arrival conditions are selected as the particular stable hyperbolic manifold trajectory at which the high thrust solution is targeted, at the crossing of the  $\pi/8$  section. Hence, boundary conditions are such that trajectories equivalent to those reported in Table 3 could be flown with low thrust propulsion technology. The complete low thrust transfer is thus defined within the region of space that was previously regarded as a two-body problem, and finishes just at the threshold distance with the three-body problem dynamics, i.e., section at  $\pi/8$  radians angular distance from Earth. Therefore, the low-thrust transfer is also modelled as in a two-body dynamical approximation, perturbed in this case only by the low thrust propulsion acceleration.

Hence, the dynamical system is defined such as:

$$\dot{\mathbf{x}} = \mathbf{f}(\mathbf{x}(t), \mathbf{T}(t), t) \quad (6)$$

where  $\mathbf{f}$  is the vector field,  $\mathbf{x}$  is the state vector and  $\mathbf{T} = [T_r, T_t, T_n]$  is the thrust vector along the radial, transversal and out-of-plane direction. The state vector  $\mathbf{x}$  is defined by means of the Gauss' form of the variational equations [40], and in order to avoid singularities near zero inclination, the nonsingular modified equinoctial elements [41],  $\{p, f, g, h, k, L, m\}$ , were used:

$$\begin{aligned}
 \dot{p} &= \frac{2p}{w} \sqrt{\frac{p}{\mu}} \cdot \frac{T_r}{m} \\
 \dot{f} &= \sqrt{\frac{p}{\mu}} \left[ \sin L \cdot \frac{T_r}{m} + \frac{1}{w} \left[ (w+1) \cos L + f \right] \cdot \frac{T_r}{m} - \frac{g}{w} (h \sin L - k \cos L) \cdot \frac{T_n}{m} \right] \\
 \dot{g} &= \sqrt{\frac{p}{\mu}} \left[ -\cos L \cdot \frac{T_r}{m} + \frac{1}{w} \left[ (w+1) \sin L + g \right] \cdot \frac{T_r}{m} - \frac{f}{w} (h \sin L - k \cos L) \cdot \frac{T_n}{m} \right] \\
 \dot{h} &= \sqrt{\frac{p}{\mu}} \frac{s^2}{2w} \cos L \cdot \frac{T_n}{m} \\
 \dot{k} &= \sqrt{\frac{p}{\mu}} \frac{s^2}{2w} \sin L \cdot \frac{T_n}{m} \\
 \dot{L} &= \sqrt{\mu p} \left( \frac{w}{p} \right)^2 + \frac{1}{w} \sqrt{\frac{p}{\mu}} (h \sin L - k \cos L) \cdot \frac{T_n}{m} \\
 \dot{m} &= -\frac{\|\mathbf{T}\|}{I_{sp} g_0}
 \end{aligned} \tag{6}$$

where  $w = \frac{p}{r} = 1 + f \cos L + g \sin L$  and  $s = 1 + h^2 + k^2$ .

The optimal control problem is now solved by finding a control law  $\mathbf{T}(t)$  and associated state history  $\mathbf{x}(t)$  that satisfies boundary conditions and path constraints (as mentioned earlier) and that minimizes a given cost function  $J$ . Since we seek to maximize the mass of the retrieved asteroid  $M_{\text{retrievable}}$ , the cost function is defined as:

$$J = -m_f \tag{6}$$

where  $m_f$  is the final mass of the asteroid-hauling spacecraft, i.e. spacecraft dry mass and asteroid  $m_f = m_{\text{dry}} + M_{\text{retrievable}}$ . The time-continuous optimal control problem is transcribed using collocation methods into a finite dimensional nonlinear programming problem (NLP), using GPOPS-II [42] software package. Finally, the NLP is solved by IPOPT [43], an open source software package using an interior point algorithm to solve large-scale NLPs [44].

When assuming high thrust propulsion systems, the retrievable mass can be straightforwardly computed by means of the rocket equation, as previously done. On the other hand, the asteroid mass  $M_{\text{retrievable}}$  that is attempted to be retrieved from a given orbit by means of a low thrust propulsion system strongly drives the feasibility of a low thrust transfer, since both maximum thrust (fixed in this case to 2 N) and time of flight are fixed. Hence, an iterative continuation process is used where the optimal control problem is solved for increasing initial asteroid-hauling spacecraft mass  $m_0$ . The continuation algorithm is initialized with initial mass  $m_0$  such that the total thrust time should be on the order of 1% of total time of flight. This initial mass  $m_0$  ensures that a first guess, as provided by the previously optimized Lambert arcs, will have a fast convergence. This mass  $m_0$  is then increased at small steps. The final convergence of this process occurs either when the full 10,000 kg of propellant have been used or, in many cases, when the spacecraft thrusts at maximum power for the full transfer time. Note that an additional constraint is added to the retrieval trajectories; the total time of flight, i.e., from departure date to arrival to the LPO, should be less than 10 years. Figure 5 shows an example of the case on which all propellant available is used within the 10 years of transfer time. This allows to retrieve a maximum asteroid mass of 340 tonnes of material. Note that in those solutions on which all the propellant cannot be used, the paper simply assumes that the unused propellant is instead asteroid material (instead of carrying ballast mass as propellant).

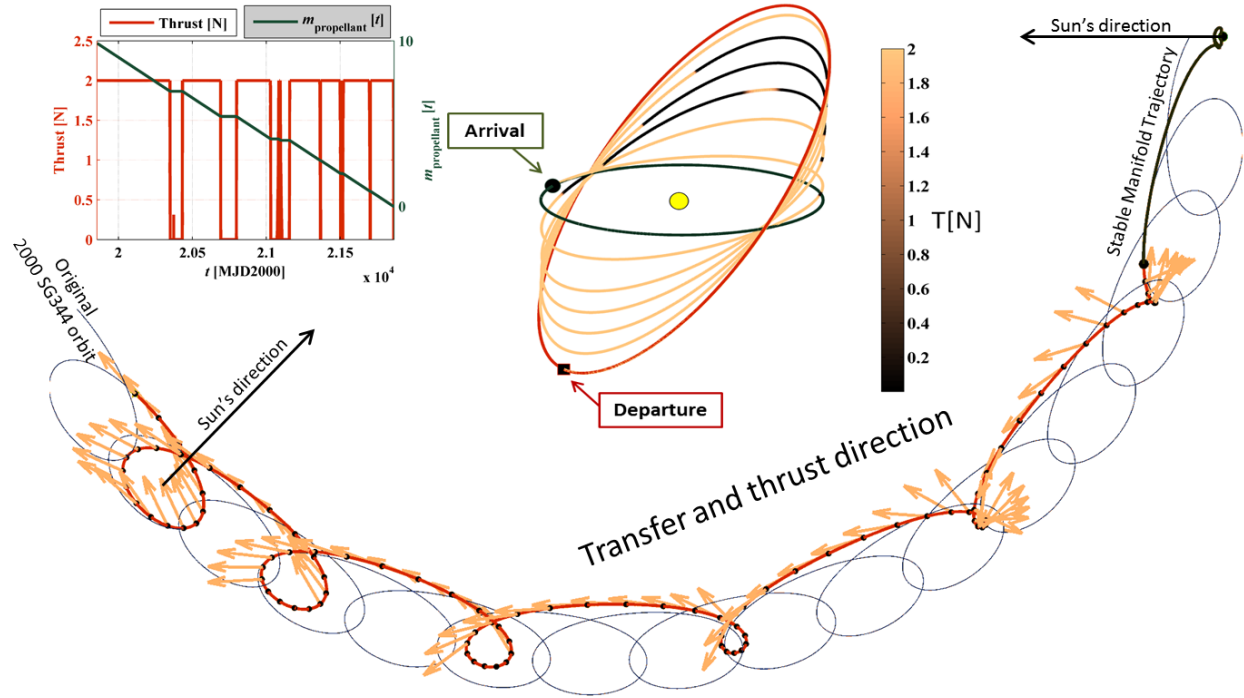


**Figure 5.** Final retrieval transfer for asteroid 2000 SG344 in both the synodic and inertial reference frame. Also, the top right corner figure shows the thrust profile and propellant mass as a function of time.

## 5.2. Asteroid Retrieval Mission Feasibility

The final results of the process described above are reported in Table 4. Among the complete database of impulsive transfer opportunities that resulted from the previous global optimization, there were all sorts of transfer opportunities with different transfer conditions but similar  $\Delta v$ . Hence, to ensure that the largest possible object was retrieved, several different transfers were optimized for each asteroid. Table 3 reports only those impulsive trajectories that yielded the maximum retrievable mass in low thrust, after the aforementioned optimal control problem and continuation process. As it can be seen in Table 3, the largest transport of asteroid mass was always achieved with a long transfer, of nearly 10 years. Hence, this is the reason why transfers in Table 3 differ slightly from those reported in Table 2, which were those minimising  $\Delta v$  and not maximizing transported mass in low thrust. The range of retrievable masses, as shown in Table 4, goes from 277 to 2,100 tonnes. For comparison, the total mass of the ISS is approximately of 450 tonnes.

**Table 4:** Asteroid retrieval mission feasibility summary for the capture trajectories in Table 3. Mission feasibility is represented with  $<M_{\min}$  if the retrievable mass  $M_{\text{retrievable}}$  is lower than the minimum asteroid mass, with  $>M_{\min}$  if  $M_{\text{retrievable}}$  is bigger than minimum asteroid mass but lower than mean mass, with  $>M_{\text{mean}}$  if  $M_{\text{retrievable}}$  is larger than mean mass and  $>M_{\max}$  if  $M_{\text{retrievable}}$  is larger than the maximum asteroid mass.

Asteroid name	Physical Properties				Isp=300s Chemical Prop.		Isp=3000s Electric Prop.	
	H	$D_{\text{range}}$ [m]	$M_{\text{range}}$ [t]	$M_{\text{mean}}$ [t]	$M_{\text{retrievable}}$ [t]	Mission Feasibility	$M_{\text{retrievable}}$ [t]	Mission Feasibility
1. 2006 RH120	29.50	2.4 - 7.5	86 - 311	105	488	$>M_{\max}$	2,100	$>M_{\max}$
2. 2007 UN12	28.70	3.4 - 10.8	259 - 941	318	140	$<M_{\min}$	973	$>M_{\max}$
3. 2011 UD21	28.50	3.8 - 11.9	342 - 1,240	420	134	$<M_{\min}$	925	$>M_{\text{mean}}$
4. 2012 TF79	27.40	6.2 - 19.7	1,562 - 5,667	1,919	95	$<M_{\min}$	739	$<M_{\min}$
5. 2010 VQ98	28.20	4.3 - 13.6	517 - 1,877	635	130	$<M_{\min}$	727	$>M_{\text{mean}}$
6. 2010 UE51	28.30	4.1 - 13.0	450 - 1,634	553	74	$<M_{\min}$	677	$>M_{\text{mean}}$
7. 2013 RZ53	31.30	1 - 3.3	7 - 26	9	91	$>M_{\max}$	595	$>M_{\max}$
8. 2008 UA202	29.40	2.5 - 7.8	99 - 358	121	70	$<M_{\min}$	576	$>M_{\max}$
9. 2011 BL45	27.00	7.5 - 23.7	2,714 - 9,849	3,335	55	$<M_{\min}$	562	$<M_{\min}$
10. 2008 EA9	27.70	5.4 - 17.1	1,032 - 3,744	1,268	72	$<M_{\min}$	556	$<M_{\min}$
11. 2015 PS228	28.80	3.3-10.3	226-819	277	62	$<M_{\min}$	536	$>M_{\text{mean}}$
12. 2009 BD	28.10	4.5 - 14.3	594 - 2,155	730	61	$<M_{\min}$	493	$<M_{\min}$
13. 2014 WX202	29.63	2.2 - 7.0	72 - 260	88	89	$>M_{\text{mean}}$	459	$>M_{\max}$
14. 2015 JD3	25.60	14.3-45.1	$19 \times 10^3$ - $68 \times 10^3$	$23 \times 10^3$	44	$<M_{\min}$	427	$<M_{\min}$
15. 1991 VG	28.50	3.8 - 11.9	342 - 1240	420	54	$<M_{\min}$	407	$>M_{\text{mean}}$
16. 2000 SG344	24.70	21.6 - 68.2	$65 \times 10^3$ - $236 \times 10^3$	$80 \times 10^3$	52	$<M_{\min}$	340	$<M_{\min}$
17. 2011 MD	28.00	4.7 -14.9	682 - 2474	838	58	$<M_{\min}$	277	$<M_{\min}$

Finally, an asteroid retrieval mission can here be said to be feasible if the maximum retrievable mass  $M_{\text{retrievable}}$  computed from the original asteroid orbit is larger than the actual mass of the asteroid. However, the mass of the asteroid, as its size, can only be inferred by the measure of its brightness in the sky, and again, this represents only an extremely rough approximation of its real mass. Knowing the absolute magnitude H of each asteroid, the diameter of the asteroid can then be computed using Eq.(6), and assuming a constant density and spherical shape the mass is given by:

$$m_{\text{ast}} = \frac{\pi}{6} \rho \left( \frac{1.329 \cdot 10^6}{\sqrt{p_v}} 10^{-H/5} [\text{m}] \right)^3 \quad (7)$$

where the asteroid's density  $\rho$  may range from  $1,300 \text{ kg/m}^3$ , for very porous objects, to  $5,300 \text{ kg/m}^3$  for metalling high-density objects [45]. However, note that both density  $\rho$  and albedo  $p_v$  depend on the object type and thus are not independent parameters. Thus, in order to obtain maximum and minimum ranges of asteroid mass, the combined parameter  $\rho(p_v)^{-3/2}$  is assumed to go from  $35,000 \text{ kg/m}^3$  for S-class asteroids to  $127,000 \text{ kg/m}^3$  for M-class, while the average NEA is assumed to have  $\rho(p_v)^{-3/2}$  of  $43,000 \text{ kg/m}^3$ . Hence, the range of asteroid plausible masses, as well as the average (~most likely) mass, are reported in Table 4. A mission feasibility flag is also used to report when the retrievable mass  $M_{\text{retrievable}}$  is above the full range of plausible asteroid masses  $M_{\text{range}}$ , above the average mass  $M_{\text{mean}}$ , above the minimum mass or below the plausible range  $M_{\text{range}}$ .

## 6. FURTHER DISCUSSION

Perhaps the most relevant result from Table 4 are the five objects (2006 RH120, 2007 UN12, 2013 RZ53, 2008 UA202 and 2014 WX202) that appear to be feasible targets for asteroid retrieval missions. Four additional objects are also likely candidates, but their real mass should be assessed accurately before their actual retrievability can be definitively discerned. These results are also extremely promising when compared with recently reported studies on the feasibility of NASA's Asteroid Redirect Robotic Mission (ARRM) [22]. Table 5 summarizes the differences between the results in the aforementioned NASA study [22] and those reported here. Note however that at least four of the objects (2013 RZ53, 2014 WX202, 2015 PS228 and 2015 JD3) had not been discovered by the time the study was performed, therefore they could not possibly be on their list. Most importantly, the methodology is inherently different; here, for example, the dynamical systems used are that of the CR3BP and the two body problem, which allows us to easily benefit from both Keplerian formulation and modern dynamical system techniques such as that of the computation of invariant manifold dynamics. NASA's work, on the other hand, considers higher fidelity dynamics that include the perturbations from Earth, Moon, Sun, Jupiter and Venus [46]. The solutions presented in this paper still require to be fed into higher fidelity dynamical models as guesses for yet another optimization process seeking the LPO dynamical substitutes in higher fidelity models. Similarly, the retrieval transfer computed here have considered only the outbound leg (Earth-to-asteroid), and assumed an average usage of 2.5 tonnes of propellant to reach the asteroid. Clearly, since the retrievable mass capability will be a strong function of the launch and return



dates, this needs to be examined in further work. Nevertheless, the purpose of comparing the data reported in [22] with that reported here (Table 4) is simply to show qualitatively the prospective benefits of targeting Sun-Earth LPOs as opposed to Earth-Moon DROs.

**Table 5:** Comparison of retrievability results as reported here and those reported in [22].

<i>Asteroid</i>	Here		ARRM [22]	
	$M_{ret}$ [t]	<i>Mission Feasib.</i>	$M_{ret}^{NASA}$ [t]	<i>Mission Feasib.</i>
2006 RH120	2,100	$>M_{max}$	490	$>M_{max}$
2008 HU4	-	-	1,600	$>M_{mean}$
2007 UN12	973	$>M_{max}$	490	$>M_{mean}$
2011 UD21	925	$>M_{mean}$	-	-
2012 TF79	739	$<M_{min}$	170	$<M_{min}$
2010 VQ98	727	$>M_{mean}$	-	-
2010 UE51	677	$>M_{mean}$	130	$<M_{min}$
2013 RZ53	595	$>M_{max}$	-	-
2008 UA202	576	$>M_{max}$	310	$>M_{mean}$
2011 BL45	562	$<M_{min}$	1,400	$<M_{min}$
2008 EA9	556	$<M_{min}$	130	$<M_{min}$
2015 PS228	536	$>M_{mean}$	-	-
2009 BD	493	$<M_{min}$	590	$<M_{min}$
2014 WX202	459	$>M_{max}$	-	-
2015 JD3	427	$<M_{min}$	-	-
1991 VG	407	$>M_{min}$	-	-
2000 SG344	340	$<M_{min}$	-	-
2011 MD	277	$<M_{min}$	690	$>M_{min}$
2012 LA	-	-	230	$<M_{min}$
2013 EC20	-	-	120	$<M_{min}$

It is clear by the results in Table 5 that targeting Sun-Earth LPOs may allow either retrieving different objects or more favourable opportunities to haul larger masses. Earth-Moon DROs also offer opportunities to retrieve objects that could have not been possibly captured into LPOs. This is by itself a very interesting result, highlighting that different capture orbits in the Earth's neighbourhood enable the capture of different asteroids, albeit with substantial overlap. The different final capture orbits may also entail different features in terms of controllability and safety. All these multi-body dynamical phenomena are highly nonlinear, thus when considering the uncertainties associated and the complexity of the mission, the different target capture orbits may offer different benefits in terms of controllability [47]. Similarly, each capture orbit entails different stability features which subsequently define characteristics such as the safety for Earth and its closest orbital environment (i.e. LEO, MEO, GEO) in terms of asteroid impact or debris generated during asteroid manipulation [48, 49].

Finally, it is also worth comparing the results computed here with those reported in Mingotti et al. [50]. Mingotti et al. targeted also 12 of the objects used here to similar capture conditions. The retrievable masses reported here for the same 12 objects are all superior to those reported in [50]. However, further analysis is required to draw conclusions on the reasons for that. The methodologies used here and in [50] are radically different, but there are also differences on the asteroid initial orbital conditions and on the system characteristics of the tugboat, or asteroid retrieval spacecraft, hence making a straightforward comparison difficult.

## 7. CONCLUSIONS

This paper has reported the latest results from AsteroidRetrieval Project (PIEF-GA-2012-330649). These show the potential of invariant manifold dynamics associated with periodic motion, and by extension also to quasi-periodic, to become an important enabler for asteroid retrieval missions. The paper reports the list of 17 asteroids, as of April 2016, that sufficiently accessible to become reasonable targets for asteroid retrieval missions. Among these, five objects (2006 RH120, 2007 UN12, 2013 RZ53, 2008 UA202 and 2014 WX202) appear to be feasible targets for asteroid retrieval missions; considering uncertainties on asteroid mass and a hypothetical space system based in current design studies for NASA's Asteroid Redirect Robotic Mission.

## Acknowledgements

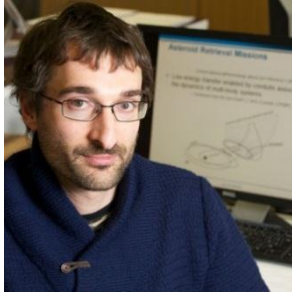
The work reported was supported by the Marie Curie grant 330649 (AsteroidRetrieval).

## References

- [1] D. Jewitt, E.D. Young, Oceans from the Skies, *Scientific American*, 312 (2015) 36-43.
- [2] Space Studies Board, Vision and Voyages for Planetary Science in the Decade 2013-2022, National Academies Press, Washington, DC, 2012.

- [3] Review of U.S. Human Spaceflight Plans Committee, HSF Final Report: Seeking a Human Spaceflight Program Worthy of a Great Nation, in, NASA, 2009.
- [4] Murdoch N. (Ed.), Asteroid Impact and Deflection Assessment (AIDA) Mission, in, 2012.
- [5] I.I. Shapiro, M. A'Hearn, F. Vilas, A.F. Cheng, F. Culbertson, D.C. Jewitt, S. Macwell, H.J. Melosh, J.H. Rothenberg, Defending Planet Earth: Near-Earth Object Surveys and Hazard Mitigation Strategies, in, National Research Council, Washington, D.C., 2010, pp. 153.
- [6] L.A. Kleiman, Project Icarus: an MIT Student Project in Systems Engineering, The MIT Press, Cambridge, Massachusetts, 1968.
- [7] D.J. Scheeres, R.L. Schweickart, The Mechanics of Moving Asteroids, in: Planetary Defense Conference, American Institute of Aeronautics and Astronautics, Orange County, California, 2004.
- [8] T.L. Edward, G.L. Stanley, Gravitational Tractor for Towing Asteroids, *Nature*, 438 (2005) 177-178.
- [9] C. Bombardelli, J. Peláez, Ion Beam Shepherd for Asteroid Deflection, *Journal of Guidance Control Dynamics*, 34 (2011) 1270-1272.
- [10] J.P. Sanchez, C. Colombo, Impact Hazard Protection Efficiency by a Small Kinetic Impactor, *Journal of Spacecraft and Rockets*, (2013) 1-14.
- [11] J.S. Lewis, Mining the sky: untold riches from asteroids, comets and planets, Helix Books/Perseus Books Reading, Massachusetts, 1996.
- [12] J.P. Sánchez, C.R. McInnes, Optimal Sunshade Configurations for Space-Based Geoengineering near the Sun-Earth L1 Point, *PLoS ONE*, 10 (2015) e0136648.
- [13] K.E. Tsiolkovsky, The Exploration of Cosmic Space by Means of Reaction Devices, *Scientific Review*, (1903).
- [14] H.-X. Baoyin, Y. Chen, J.-F. Li, Capturing near earth objects, *Research in Astronomy and Astrophysics*, 10 (2010) 587-598.
- [15] J.P. Sanchez, C.R. McInnes, Asteroid Resource Map for Near-Earth Space, *Journal of Spacecraft and Rockets*, 48 (2011) 153-165.
- [16] Z. Hasnain, C. Lamb, S.D. Ross, Capturing near-Earth asteroids around Earth, *Acta Astronautica*, 81 (2012) 523-531.
- [17] C. Lewicki, P. Diamandis, E. Anderson, C. Voorhees, F. Mycroft, Planetary Resources—The Asteroid Mining Company, *New Space*, 1 (2013) 105-108.
- [18] J.-P. Sanchez, C. McInnes, Available Asteroid Resources in the Earth's Neighbourhood, in: V. Badescu (Ed.) *Asteroids*, Springer Berlin Heidelberg, 2013, pp. 439-458.
- [19] G. Gómez, W.S. Koon, M.W. Lo, J.E. Marsden, J. Masdemont, S.D. Ross, Invariant Manifolds, the Spatial Three-Body Problem and Space Mission Design, in: *AIAA/AAS Astrodynamics Specialist Meeting*, Quebec City, Quebec, Canada, 2001.
- [20] J. Brophy, F. Culick, L. Friedman, C. Allen, D. Baughman, J. Bellerose, et al., Asteroid Retrieval Feasibility Study, in, Keck Institute for Space Studies, California Institute of Technology, Jet Propulsion Laboratory, Pasadena, California, 2012.
- [21] D. García Yárnoz, J.P. Sanchez, C.R. McInnes, Easily retrievable objects among the NEO population, *Celestial Mechanics and Dynamical Astronomy*, (2013) 1-22.
- [22] B.K. Muirhead, J.R. Brophy, Asteroid Redirect Robotic Mission feasibility study, in: *Aerospace Conference*, 2014 IEEE, 2014, pp. 1-14.
- [23] E. Belbruno, B.G. Marsden, Resonance Hopping in Comets, *Astronomical Journal*, 113 (1997) 1433-1444.
- [24] W.S. Koon, M.W. Lo, J.E. Marsden, S.D. Ross, Heteroclinic Connections Between Periodic Orbits and Resonance Transitions in Celestial Mechanics, *Chaos*, 10 (2000) 427-469.
- [25] Y. Ren, J.J. Masdemont, G. Gómez, E. Fantino, Two mechanisms of natural transport in the Solar System, *Communications in Nonlinear Science and Numerical Simulation*, 17 (2012) 844-853.
- [26] W.S. Koon, M.W. Lo, J.E. Marsden, S.D. Ross, *Dynamical systems, the three-body problem and space mission design*, Marsden Books, 2008.
- [27] V. Szebehely, *Theory of orbits*, Academic Press, New York, 1967.
- [28] K.C. Howell, Families of Orbits in the Vicinity of Collinear Libration Points, *Journal of the Astronautical Sciences*, 49 (2001) 107-125.
- [29] G. Gómez, J. Llibre, R. Martínez, C. Simó, *Dynamics and Mission Design Near Libration Point Orbits—Fundamentals: The Case of Collinear Libration Points*, World Scientific, Singapore, 2000.
- [30] C. Simó, G. Gómez, J. Llibre, R. Martínez, J. Rodríguez, On the optimal station keeping control of halo orbits, *Acta Astronautica*, 15 (1987) 391-397.
- [31] K.C. Howell, H.J. Pernicka, Stationkeeping Methods for Libration Point Trajectories, *Journal of Guidance Control Dynamics*, 16 (1993) 151-159.

- [32] D.J. Dichmann, C.M. Alberding, W.H. Yu, Stationkeeping Monte Carlo Simulation for the James Webb Space Telescope, in: International Symposium on Space Flight Dynamics 2014, Laurel, MD; United States, 2014.
- [33] M.W. Lo, S.D. Ross, The Lunar L1 Gateway: Portal to the Stars and Beyond, in: AIAA Space 2001 Conference, Albuquerque, New Mexico, 2001.
- [34] E. Canalias, J. Masdemont, Homoclinic and heteroclinic transfer trajectories between planar Lyapunov orbits in the sun-earth and earth-moon systems, *Discrete and Continuous Dynamical Systems - Series A*, 14 (2006) 261 - 279.
- [35] J.P. Sanchez, C.R. McInnes, On the Ballistic Capture of Asteroids for Resource Utilization, in: 62nd International Astronautical Congress, International Astronautical Federation, Cape Town, SA, 2011.
- [36] M. Vasile, M. Locatelli, A Hybrid Multiagent Approach for Global Trajectory Optimization, *Journal of Global Optimization*, 44 (2009) 461–479.
- [37] E. Bowell, B. Hapke, D. Domingue, K. Lumme, J. Peltoniemi, A.W. Harris, Application of photometric models to asteroids, in: R.P. Binzel, R.P. Gehrels, M.S. Matthews (Eds.) *Asteroids II*, Univ. of Arizona Press, Tucson, 1989, pp. 524–556.
- [38] W.H. Alan, The H-G Asteroid Magnitude System: Mean Slope Parameters, *Lunar and Planetary Science*, 20 (1989) 375-376.
- [39] S. Kitamura, Y. Ohkawa, Y. Hayakawa, H. Yoshida, K. Miyazaki, Overview and research status of the JAXA 150-mN ion engine, *Acta Astronautica*, 61 (2007) 360-366.
- [40] R.H. Battin, *Introduction to the Mathematics and Methods of Astrodynamics* American Institute of Aeronautics and Astronautics, Reston, Virginia, 1999.
- [41] M.J.H. Walker, B. Ireland, J. Owens, A set modified equinoctial orbit elements, *Celestial mechanics*, 36 (1985) 409-419.
- [42] M.A. Patterson, A.V. Rao, GPOPS-II: A MATLAB Software for Solving Multiple-Phase Optimal Control Problems Using hp-Adaptive Gaussian Quadrature Collocation Methods and Sparse Nonlinear Programming, *ACM Trans. Math. Softw.*, 41 (2014) 1-37.
- [43] A. Wächter, L.T. Biegler, On the implementation of an interior-point filter line-search algorithm for large-scale nonlinear programming, *Mathematical Programming*, 106 (2006) 25-57.
- [44] A. Wächter, An interior point algorithm for large-scale nonlinear optimization with applications in process engineering, in: PhD thesis, Carnegie Mellon University, Pittsburgh, PA, USA, 2002.
- [45] S.R. Chesley, P.W. Chodas, A. Milani, D.K. Yeomans, Quantifying the Risk Posed by Potential Earth Impacts, *Icarus*, 159 (2002) 423-432.
- [46] N. Strange, D. Landau, T. McElrath, G. Lantoine, T. Lam, Overview of mission design for NASA Asteroid Redirect Robotic Mission concept, in: N.A.a.S.A. Jet Propulsion Laboratory (Ed.) 33rd International Electric Propulsion Conference (IEPC2013), Washington, D.C., October 6-10, 2013, 2013.
- [47] M. Ceriotti, J.P. Sanchez Control of Asteroid Retrieval Trajectories to Libration Point Orbits, *Acta Astronautica*, (In Press).
- [48] E.M. Alessi, The reentry to Earth as a valuable option at the end-of-life of Libration Point Orbit missions, *Advances in Space Research*, 55 (2015) 2914-2930.
- [49] J. Roa, C.J. Handmer, Quantifying hazards: asteroid disruption in lunar distant retrograde orbits, *arXiv preprint arXiv:1505.03800*, (2015).
- [50] G. Mingotti, J.P. Sánchez, C.R. McInnes, Combined low-thrust propulsion and invariant manifold trajectories to capture NEOs in the Sun–Earth circular restricted three-body problem, *Celestial Mechanics and Dynamical Astronomy*, 120 (2014) 309-336.

**VITAE****JOAN PAU SANCHEZ**

Dr. Joan-Pau Sánchez studied physics at the Universitat de Barcelona, and an MSc in Mission Analysis and Design at the University of Glasgow. He was awarded his PhD also from University of Glasgow in 2009, after completing a comprehensive analysis of deflection alternatives against Earth-threatening asteroids. He then briefly worked as space mission analyst at GMV Aerospace and Defence, before returning to academia. He joined the University of Strathclyde as postdoctoral research fellow, leading the Visionary Space Systems theme within the ERC project VISIONSPACE. In 2012, he was granted an individual Marie Curie Fellowship to pursue his research on asteroid retrieval missions at the Universitat Politècnica de Catalunya. He joined Cranfield University on February 2015 as lecturer in Space Engineering. He is particularly active in the research fields of small body missions and space macro engineering projects.

**DANIEL GARCÍA-YÁRNOZ**

After graduating in aerospace engineering from the Technical University of Madrid in 2002, Daniel García Yárnoz joined the Spain-based company GMV as space mission analyst and worked in the areas of orbital mechanics, formation flying, satellite constellations and reusable launch vehicles. From 2004 he worked for 7 years at ESA/ESOC as GMV contractor in the mission analysis section. At ESOC he has been involved in future interplanetary missions to Mercury, Mars and Jupiter moons, as well as various other small feasibility studies. Daniel then became a PhD researcher at the University of Strathclyde in October 2011, focusing on the dynamics of minor bodies, and the study of novel ways of manipulating small Near Earth Asteroids. He was awarded a PhD for this research work on 2015. Following his PhD, Daniel briefly worked for 6 months at ISAS/JAXA on small missions to the Moon and asteroids.

Highlights:

- This paper summarizes the final results of the EU-funded ASTEROIDRETRIEVAL Project.
- Low thrust trajectories to retrieve 17 of the closest asteroids are presented.
- These retrieval trajectories are enabled by hyperbolic invariant manifold dynamics.
- Five asteroids appear to be feasible targets for asteroid retrieval missions.
- These are; 2006 RH120, 2007 UN12, 2013 RZ53, 2008 UA202 and 2014WX202.

Accepted manuscript

2016-06-16

# Asteroid retrieval missions enabled by invariant manifold dynamics

Sanchez, Joan-Pau

Elsevier

---

Joan Pau Sanchez, Daniel Garcia Yáñez, Asteroid retrieval missions enabled by invariant manifold dynamics, *Acta Astronautica*, Vol. 127, pp. 667-677

<http://dx.doi.org/10.1016/j.actaastro.2016.05.034>

*Downloaded from Cranfield Library Services E-Repository*